II International Conference on Particle-based Methods - Fundamentals and Applications
PARTICLES 2011
E. Oñate and D.R.J. Owen (Eds)

A DISCRETE ELEMENT APPROACH IN FRACTURE MECHANICS OF BRITTLE MATERIALS

BA DANH LE, GEORG KOVAL AND CYRILLE CHAZALLON

Laboratory of Engineering Design (LGECO)
National Institute of Applied Sciences of Strasbourg (INSA de Strasbourg)
24, Boulevard de la Victoire 67084 Strasbourg, France
e-mail: georg.koval@insa-strasbourg.fr

Key words: fracture mechanics, DEM, brittle materials

Abstract. In this study, we use the discrete element method (DEM) to model the fracture behavior of brittle materials in 2D. The material consists of a set of particles in contact with a close-packed structure. It allows us to derive an expression for the stress intensity factor as a function of the contact forces near the crack tip. A classical failure criterion, based on the material's toughness, is then adopted in the analysis of mixed mode crack propagation, represented by the contact loss between particles. We compare our model to classical solutions of tensile crack (mode I) and shear crack (mode II).

1 INTRODUCTION

The discrete element method (DEM) [1] is generally used in contact problems of a large number of particles. Material properties like elasticity, plasticity, viscosity, etc. can be modeled with different contact laws between particles. The introduction of bonded contacts with a limited resistance allow us to model brittle materials in fracture problems [2]. Although realistic macroscopic brittle behaviors are obtained with these models, a previous calibration of the contact laws is required [3].

Recent work of [4] presents analytical expressions which relate directly DEM material parameters to elastic continuous solid parameters (i.e. Young's modulus and Poisson's ratio). These expressions are based on a bidimensional close-packed assembly of particles. Considering this equivalence between discrete and continuous models in elasticity, we propose a DEM approach in fracture mechanics for brittle materials. The concordance with continuous classical theories exempt us of any previous calibration of the model parameters in order to attain convergent results.

This article begins with a presentation of the elastic contact law adopted in our simulations in Sec. 2. In Sec. 3, we present the theoretical elements of our discrete model in fracture mechanics. We compare our numerical results to classical cases of tensile and shear fracture in Sec. 4. Finally we present the conclusions of the work.

2 DEM IN ELASTICITY

Let us consider an homogenous (elastic and isotropic) material as an assembly of particles in contact. All mechanical properties of these particles are defined at the contact level (a local scale). The stresses are transmitted through contact forces, while material strain depends on particles translational and rotational motions.

2.1 Contact forces

We adopt a linear relation between contact forces and relative particle position which can be seen as a simplified version of Hertz contact model. Each force f_{ij} (applied by a particle j over a particle i) is decomposed in normal and tangential components. Let us define $\overrightarrow{n}_{ij}$ as the normal vector pointing from the center of i to the center of j and $\overrightarrow{t}_{ij}$ as the tangential vector, orthogonal to $\overrightarrow{n}_{ij}$ and positively oriented (see Fig. 1).

The normal component is the sum of two contributions $\overrightarrow{f}_{nij} = \overrightarrow{f}^{e}_{nij} + \overrightarrow{f}^{v}_{nij}$. The elastic one, $\overrightarrow{f}^{e}_{nij} = k_n \delta_n \overrightarrow{n}_{ij}$, depends on the normal deflection δ_n and the normal stiffness k_n. The inelastic one, $\overrightarrow{f}^{v}_{nij} = c_n \dot{\delta_n} \overrightarrow{n}_{ij}$ depends on a viscous damping parameter c_n and the time derivative of the normal deflection $\dot{\delta_n}$. The latter contribution is only introduced to stabilize the numerical integration scheme. We choose c_n as a small fraction of $\sqrt{mk_n}$ (where m is the particle mass) which guarantees a negligible inelastic effect.

The (elastic) tangential component $\overrightarrow{t}_{ij} = k_t \delta_t \overrightarrow{t}_{ij}$ depends only on tangential relative displacement δ_t and tangential stiffness k_t.

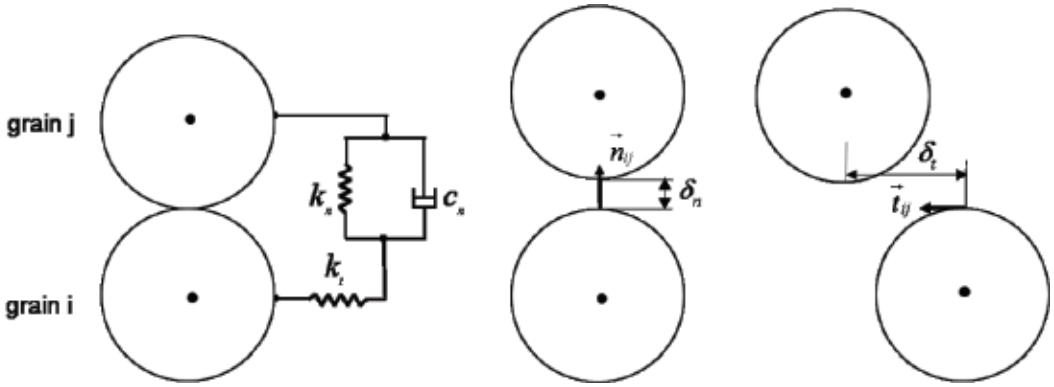

Figure 1: Contact model between two particles.

2.2 Particle displacement and elastic behavior

The numerical approach is based on molecular dynamics method like in [1, 5]. The discrete particle motion equations are solved by Gear's order three predictor-corrector algorithm [6].

A macroscopic strain tensor can be derived from particle displacements. The balance of the contact forces gives rise to a macroscopic stress tensor. Associating this equivalence between continuous and discrete approaches, [4] has shown that normal and tangential stiffness (k_n and k_t, respectively) can be directly related to elasticity parameters of the continuous solid (Young's modulus E and Poisson's ration ν, for example).

3 DEM IN FRACTURE MECHANICS

In this section, we explore the similarity between discrete and continuous approaches in elasticity in order to derive expressions for the intensity factors in our discrete model. Based on these results, we deduce a crack propagation criterion for brittle materials in mixed mode.

3.1 Stress field near a crack tip

The singular stress field near a crack tip (in polar coordinates, see Fig. 2) can be written as in [7]:

$$\begin{aligned}
\sigma_{rr}(r,\theta) &= \frac{K_{rr}(\theta)}{\sqrt{2\pi r}} \Rightarrow K_{rr}(\theta) = K_I \cos\frac{\theta}{2}\left(1+\sin^2\frac{\theta}{2}\right) + K_{II}\left(-\frac{5}{4}\sin\frac{\theta}{2}+\frac{3}{4}\sin\frac{3\theta}{2}\right),\\
\sigma_{\theta\theta}(r,\theta) &= \frac{K_{\theta\theta}(\theta)}{\sqrt{2\pi r}} \Rightarrow K_{\theta\theta}(\theta) = K_I \cos\frac{\theta}{2}\left(1-\sin^2\frac{\theta}{2}\right) + K_{II}\left(-\frac{3}{4}\sin\frac{\theta}{2}-\frac{3}{4}\sin\frac{3\theta}{2}\right), \quad (1)\\
\sigma_{r\theta}(r,\theta) &= \frac{K_{r\theta}(\theta)}{\sqrt{2\pi r}} \Rightarrow K_{r\theta}(\theta) = K_I \sin\frac{\theta}{2}\cos^2\frac{\theta}{2} + K_{II}\left(\frac{1}{4}\cos\frac{\theta}{2}+\frac{3}{4}\cos\frac{3\theta}{2}\right),
\end{aligned}$$

where K_I and K_{II} are the stress intensity factors [8]. K_I is associated to opening mode, while K_{II}, to shear mode. Their values, which depend on loading and crack shape, quantify the strength of the singularity. For brittle materials they are directly associated to the energy release rate during crack extension [9].

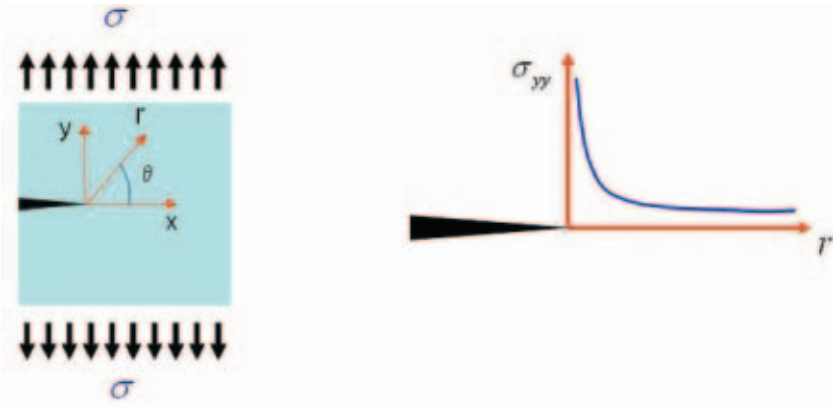

Figure 2: Crack tip and singular stress field.

3.2 Mixed mode crack propagation - Maximum circumferential tensile stress

Presented by [10], this simple criterion for fracture propagation depends only on the knowledge of the stress state near the tip of a crack. This theory states that crack propagates in the plane perpendicular to the direction of greatest tension θ_0 ($\sigma_{r\theta}(r, \theta_0) = 0$, or simply $K_{r\theta}(\theta_0) = 0$) when $K_{\theta\theta}(\theta_0) = K_{IC}$ (where K_{IC} is the material toughness) [11].

3.3 Stress intensity factor $K_{\theta\theta}$ on the discrete approach

In our discrete approach, a crack may be represented by the absence of contact forces between some close particles, like the example in Fig. 3. The crack propagation is consequently modeled with the suppression of contact forces. So as to determine which contact should be suppressed, we seek the maximum value of $K_{\theta\theta}(\theta)$.

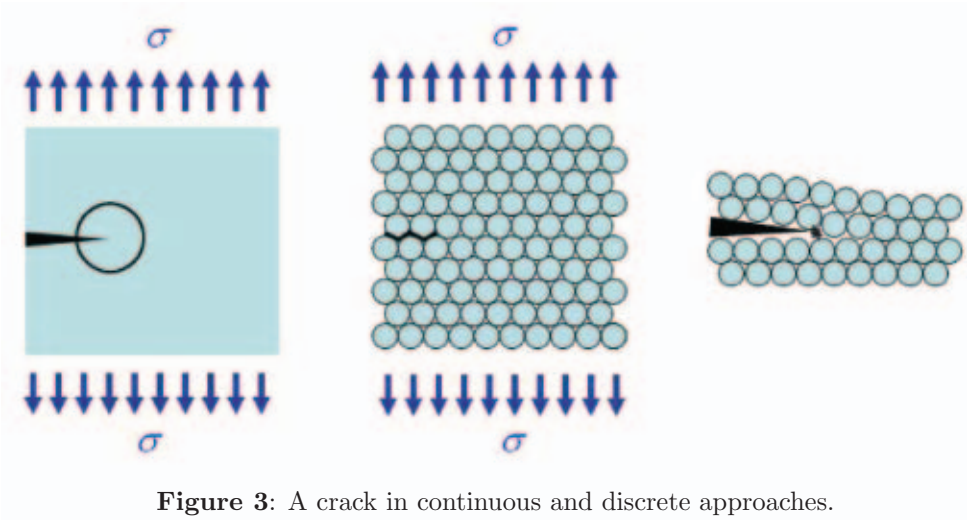

Figure 3: A crack in continuous and discrete approaches.

Let us consider a potential segment (composed by two consecutive contacts: ik and jk) in a given direction θ next to a crack tip (see Fig. 4). Taking into account the contact forces acting over particles i and j, the resultant force in θ direction is equal to:

$$f'_\theta = \overrightarrow{f}_{nik} \sin\alpha + \overrightarrow{f}_{tik} \cos\alpha + \overrightarrow{f}_{njk} \cos\alpha - \overrightarrow{f}_{tjk} \sin\alpha, \tag{2}$$

where $\overrightarrow{f}_n$ and $\overrightarrow{f}_t$ are normal and tangential contact forces respectively, and $\alpha = \pi/3$.

The resultant force f_θ might equilibrate the effect of $\sigma_{\theta\theta}$ (Eq. 1) along a straight distance d, where d is the diameter of the particles (as can be seen in Fig. 4):

$$f_\theta = \int_0^d \sigma_{\theta\theta} dr = \int_0^d \frac{K_{\theta\theta}(\theta)}{\sqrt{2\pi r}} dr = \sqrt{\frac{2d}{\pi}} K_{\theta\theta}(\theta). \tag{3}$$

The force f'_θ converges to f_θ for decreasing values of d. The comparison of Eqs. 2 and 3 leads to the approximation of the stress intensity factor $K_{\theta\theta}(\theta)$ as a function of contact forces in discrete approach:

$$K_{\theta\theta}(\theta) \approx \left[\left(\overrightarrow{f}_{nik} + \overrightarrow{f}_{njk} \right) \frac{\sqrt{3}}{2} + \left(\overrightarrow{f}_{tik} - \overrightarrow{f}_{tjk} \right) \frac{1}{2} \right] \sqrt{\frac{\pi}{2d}}. \tag{4}$$

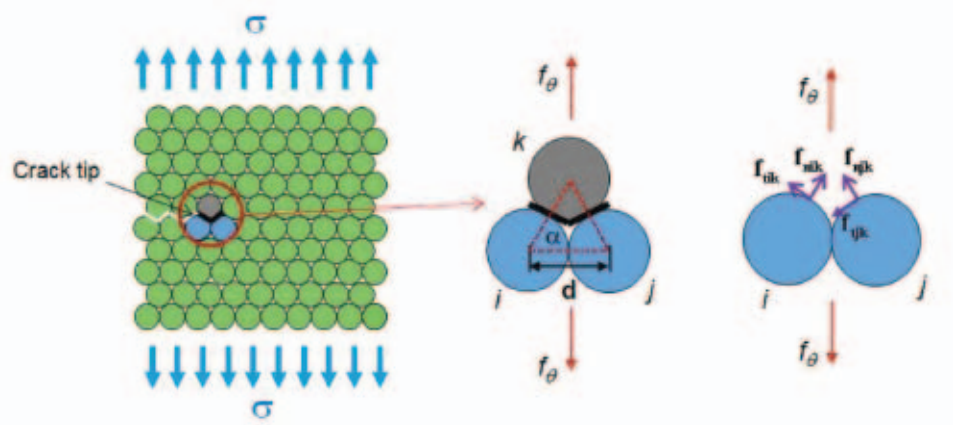

Figure 4: Potential propagation segment in the discrete approach and corresponding contact forces.

Therefore a systematic analysis of all contact pairs allow the identification of the points that are susceptible to cracking. At a given segment, if the stress intensity $K_{\theta\theta}(\theta)$ reaches the material toughness value K_{IC}, the most tensioned contact (between $\overrightarrow{f}_{nik}$ and $\overrightarrow{f}_{njk}$) is suppressed and the crack propagates.

4 COMPARISON TO CLASSICAL RESULTS

In this section we compare our numerical results to classical solutions of fracture mechanics of brittle materials. Two situations are analyzed: pure tensile fracture (mode I) and pure (initial) shear fracture (mode II) in plane stress.

We suppose for simplicity that the particle diameter d also corresponds to the thickness of the simulated bidimensional elements without loss of generality. The units of length and mass are respectively: d and the particle mass m. This implies (for a given material toughness K_{IC}) $T = \sqrt{m/(K_{IC}\sqrt{d})}$ as time unit and $K_{IC}/\sqrt{d}$ as stress unit. Small strains are modeled taking $k_n = 10^4 K_{IC}/\sqrt{d}$ as normal stiffness. The ratio between tangential and normal stiffness $k_t/k_n = 0.5$ (directly related to Poisson ratio) has no fundamental effect in plane stress results. We adopt a small value of viscous damping $c_n = 0.65\sqrt{mK_{IC}\sqrt{d}}$.

4.1 Tensile fracture

We present the results for two pre-cracked samples following the schemes presented in Fig. 5 (middle-crack tension panel) and Fig. 6 (double edge notch tension panel). A

vertical displacement induces a mean tensile stress σ to the sample. We measure the maximum stress value σ_{max} supported by the structure before complete fracture. The panels have a rectangular shape with height equal to 3 times width to avoid eventual boundary effects.

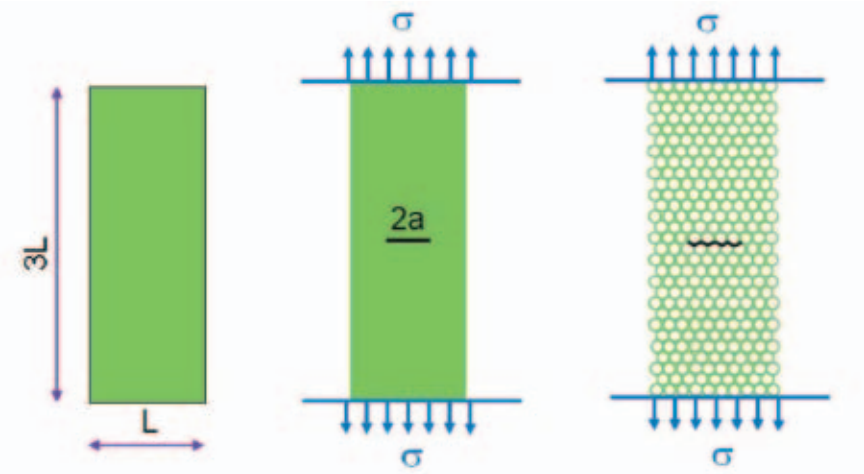

Figure 5: Tensile test - middle-crack panel.

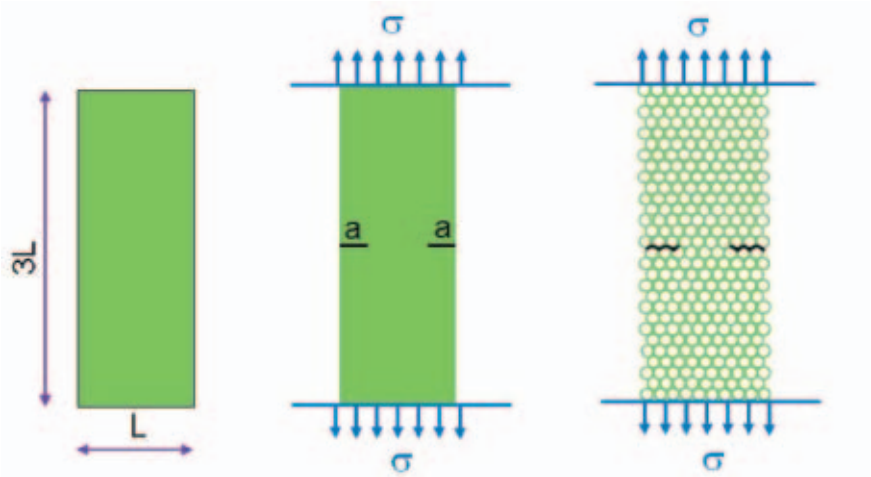

Figure 6: Tensile test - double edge notch panel.

Our numerical results of σ_{max} are compared to the following expressions [7]:
- middle-crack tension panel

$$\sigma_{max} = \frac{K_{IC}}{\sqrt{\pi a}} \left[1 + 0.256(a/L) - 1.152(a/L)^2 + 12.22(a/L)^3\right]^{-1}, \tag{5}$$

- double edge notch tension panel

$$\sigma_{max} = \frac{K_{IC}}{\sqrt{\pi a}} \left[1.12 + 0.43(a/L) - 4.79(a/L)^2 + 15.46(a/L)^3\right]^{-1}. \quad (6)$$

In both cases, four different crack lengths a/L were tested: 3/22, 4/22, 5/22, and 6/22. The maximum stress σ_{max} supported by the panels before fracture propagation decreases when crack length grows as shown in Fig. 7. The systematic variation of the ratio L/d allows the analysis of the discrete approach convergence. Higher values of L/d are associated to more precise descriptions of the crack zone inducing better results whatever the crack type.

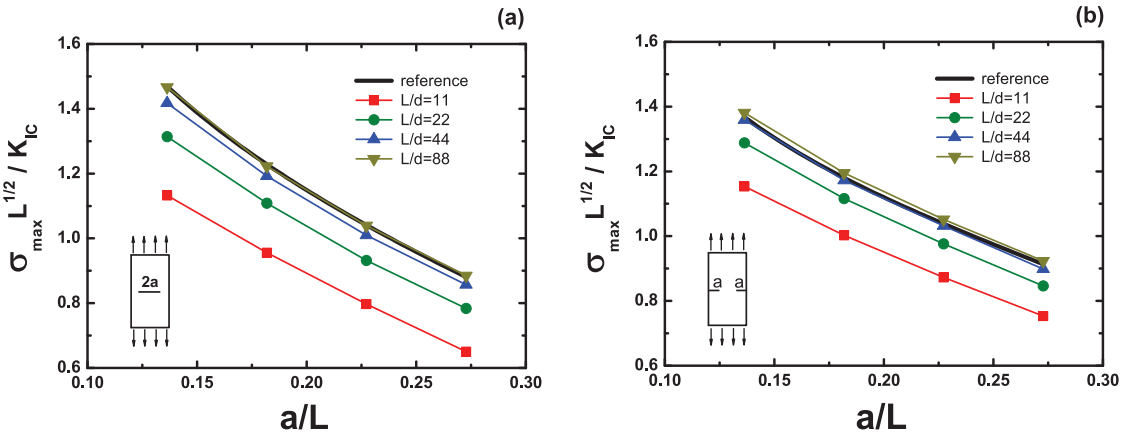

Figure 7: Normalized maximum stress $\sigma_{max}\sqrt{L}/K_{IC}$ as a function of the crack length a/L for the (a) middle-crack and (b) double edge notch panels.

In order to verify any eventual effect of the particle disposition on the results, we have also tested samples with an orthogonal orientation (compared to Fig. 3). A similar convergence (compared to Fig. 7) indicates the generality of the Eq. 4 with respect to the direction.

4.2 Shear fracture

Shear stress may induce crack branching under certain conditions. Let us consider a square plate (side length L) under biaxial stresses (lateral compression σ_x and vertical tension σ_y) with an initial inclined crack of length a (see Fig. 8). Depending on the initial crack angle α, a pure shear stress condition (in α direction) can be obtained if $\sigma_x/\sigma_y = \tan^2\alpha$. Following the maximum circumferential tensile stress criterion (Sec. 3.2), for pure shear stress ($K_I = 0$), the angle which maximizes $\sigma_{\theta\theta}$ (Eq. 1) is $\theta_0 = 70.5^o$ (relative to α). The crack branching angle θ_0 is only a prediction of the initial crack propagation. The general tendency of the crack is to become horizontal, orthogonal to stress tensile direction.

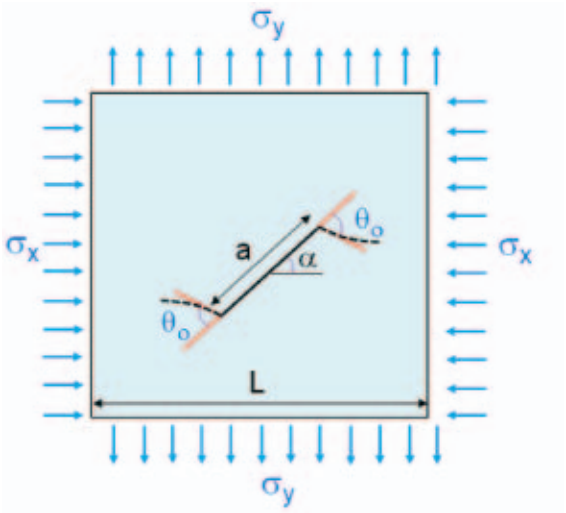

Figure 8: Square plate with an inclined crack under biaxial loading. The dotted lines indicate the crack propagation path.

The results of the simulation of an inclined crack with $\alpha = 60^o$, $a/L = 0.41$, $L/d = 176$ are shown in Fig. 9. The crack propagation presents a coherent path tending slightly to an horizontal direction (see Fig. 9a). In detail, at Fig. 9b, the theoretical prediction of the initial crack branching is fairly obtained.

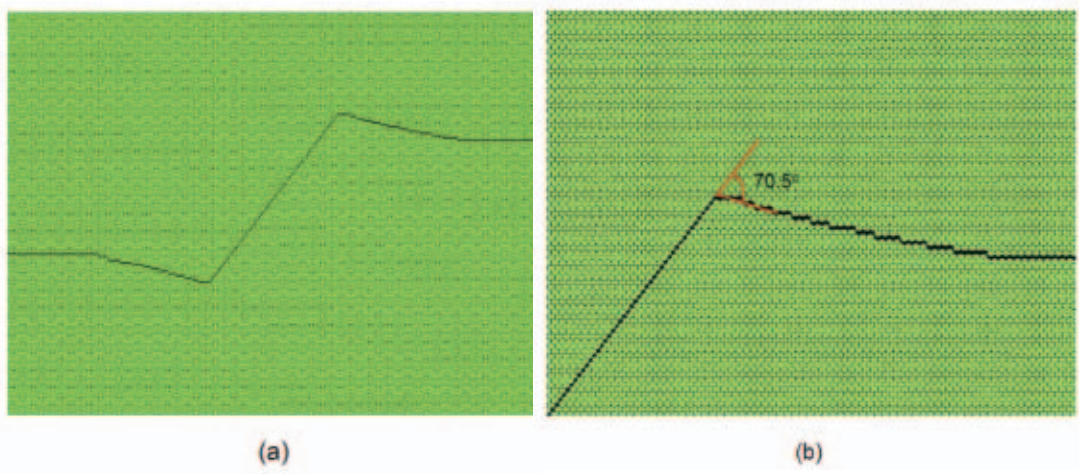

Figure 9: (a) Simulated inclined crack under biaxial load. In detail, (b) the theoretical prediction of the crack branching.

5 CONCLUSIONS

We propose in this article DEM approach in fracture mechanics of isotropic brittle materials entirely compatible with continuous classical theory. Based on the equivalence

between discrete and continuous approaches in elasticity, we present an expression for the stress intensity factor $K_{\theta\theta}$ (in polar coordinates) as a function of the forces of two adjacent contacts. The well known "maximum circumferential tensile stress" criterion for mixed mode crack propagation is then associated to allow the study of complex plane cracks. The toughness of the material is directly introduced as a model parameter without any previous calibration, which represents an important feature.

The simplicity of the formulation is followed by encouraging numerical results. The DEM approach is compared to two tensile cases (mode I); both presenting a monotone convergence towards classical solutions for more precise discretization (evaluated by the ratio L/d). The effect of shear stresses (mode II) is analyzed through a biaxial test of a sample with an initial inclined crack. The initial crack branching follows the theoretical prediction as well as the general evolution of the crack.

As perspective, we consider the study of interfacial cracks (between different materials) and the effect of compression loading (with crack closure). Both cases can easily be implemented for multiple cracks with DEM methods.

REFERENCES

[1] Cundall, P. A. and Strack, O. D. L. A discrete numerical model for granular assemblies. *Gotech.* (1979) **29**:47–65.

[2] Potyondi, D. and Cundall, P. A bonded-particle model for rock. *Int. J. Rock Mech. Min. Sci.* (2004) **41(8)**:1329–1364.

[3] Schöpfer, M. P. J., Steffen, A., Childs, C. and Walsh, J. The impact of porosity and crack density on the elasticity, strength and friction of cohesive granular materials: Insight from dem modelling. *Int. J. Rock Mech. Min. Sci.* (2009) **46**:250–261.

[4] Tavarez, F. A. and Plesha M., Discrete element method for modelling solid and particulate materials, *International journal for numerical methods in engineering* (2007) **70**:379–404.

[5] Koval, G., Roux, J.-N., Corfdir, A. and Chevoir, F. Annular shear of cohesionless granular materials: From the inertial to quasistatic regime, *Phys. Rev. E* (2009) **79(2)**:021306.

[6] Allen, M. P. and Tildesley, D. J. *Computer Simulation of Liquids*, Oxford University Press, Oxford, (1987).

[7] Saouma, V. *Fracture mechanics*, Lecture notes, (2000).

[8] Irwin, G. Analysis of stresses and strains near the end of a crack traversing a plate, *Journal of Applied Mechanics* (1957) **24**:361–364.

[9] Chaboche, J. L. and Lemaitre, J. *Mécanique des matériaux solides*, Dunod, (1984).

[10] Erdogan, F. and Sih, G. C. Crack extension in plates under plane loading and transverse shear, *J. Basic Eng.* (1963) **85**:519–527.

[11] Labbens, R. *Introduction à la mécanique de la rupture*, Éditions Pluralis, (1980).